2009 IEEE 11th International Conference on Rehabilitation Robotics
Kyoto International Conference Center, Japan, June 23-26, 2009

Precise Position and Trajectory Control of pneumatic Soft-Actuators for Assistance Robots and Motion Therapy Devices

Mathias Jordan, Dennis Pietrusky, Miroslav Mihajlov, Oleg Ivlev

Abstract—**The goal of this work is the development and performance analysis of control algorithms for new soft fluidic actuators with rotary elastic chambers (REC-actuators). Due to their inherent compliancy these actuators fulfill the requisites for building intrinsically safe mechanisms as assistance robots and motion therapy devices, working in direct physical contact with humans. Besides the difficulties common for control design of pneumatic systems, these actuators itself posses several nonlinear characteristics causing specific problems in their modeling and control. In this work the decentralized joint control scheme is implemented, where the position controller has a cascade structure with a non-linear model based pressure control in the inner loop. Two different position control approaches, which require minimal information on the dynamics of the actuator mechanical subsystem, were investigated and tested: sliding mode control with time delay estimation as well as a fuzzy control with parameter optimization based on genetic algorithms.**

I. Introduction

In service and assistance applications robotic arms are increasingly making use of specific features of soft, i.e. inherently compliant actuators. These actuators fulfill the requisites for building intrinsically safe mechanisms which cannot be achieved by solely use of feedback force control in combination with a stiff (typically electric with high transmission) actuator. Besides controllable compliance, high power/weight and power/volume ratios combined with torque generation of some tens of Newton-meters are needed actuator performances for robots working in direct physical contact with humans.

Rotary actuator with Elastic Chambers (REC-actuator), as a kind of fluidic muscle, has been recently developed aiming at inherently compliant compact rotary joints intended for robots working in human environment, especially in assistive and rehabilitation tasks [1],[2]. The key feature of the actuator design is the use of special rotary elastic chambers antagonistically arranged, with a similar working principle to the single vane type fluid motors. Due to their design, these actuators can be integrated in the revolute robotic joint directly, without any additional transmission elements, leading to more efficient and simpler robotic arm construction compared to those built by linear fluidic muscles. Some characteristics of soft fluidic actuators are similar to those of natural muscles, enabling an antagonistic pair of these actuators to vary the stiffness independent of position/force control. These properties make them especially suitable for assistance robots as well as for motion therapy devices with assistive behavior during the therapy depending on a patient activity [3], [4].

All types of soft fluidic actuators are characterized with complex nonlinear dynamics making robust and precise control a difficult task. Besides the difficulties common for control design of pneumatic systems, these actuators itself posses several nonlinear characteristics causing specific problems in their modeling and control. We previously reported the results of position and pressure control design for the pneumatic REC-actuator with switching valves in [5], [6]. The high level of noise produced by the PWM controlled switching valves is however unacceptable especially for assisting tasks using motion therapy devices.

In this paper, results of position and pressure control of pneumatic soft actuators using flow-proportional valves providing less noise at higher flow rates are reported. Two different position control approaches were investigated and compared: sliding mode control with time delay estimation and the fuzzy control with parameter optimization based on genetic algorithms.

II. Working Principle and Experimental Setups

The working principle of the REC-actuators is analogous to conventional single vane fluidic motor, which consists of two vanes, one fixed in a motor case and a moving one with gasket. The vanes shape two working chambers in a motor case. An essential constructional difference in the design of the soft rotary actuators is in the use of elastic chambers that replace the rigid chambers of the conventional vane actuator. A hermetic, hard and heavy motor case is not needed anymore. When pressurized, the rotary elastic chamber expands in meridian direction mainly and contracts when depressurized.

Two rotary inherent compliant (soft) joint modules, R100 and R90, realizing this working principle, were developed and here used in the experimental setups, which can be seen

Manuscript received April 23, 2009. This work has been supported by the German Federal Ministry of Education and Research (BMBF) through the grants 16SV2290 and 01EZ0769

M. Jordan is with the University of Bremen, Institute of Automation, Otto-Hahn-Allee, NW1, D-28359 (e-mail:mathias.jordan@gmx.net).

D. Pietrusky was with the University of Bremen. He is now with the Daimler AG, D-21160 Hamburg (e-mail: mail@dpietrusky.de).

M. Mihajlov was with the University of Bremen and with the FWBI Friedrich-Wilhelm-Bessel-Institute Research Company, Bremen. He is now with the ITK Engineering AG, D-70565 Stuttgart (e-mail: mihajlov@iat.uni-bremen.de).

O. Ivlev is with the FWBI Friedrich-Wilhelm-Bessel-Institute Research Company, Bremen and with the University of Bremen, Institute of Automation, Otto-Hahn-Allee, NW1, D-28359 Bremen (phone: +49421-218-3217; fax: +49421-218-4816; e-mail: ivlev@fwbi-bremen.de).

in Fig. 1,2. Basing on the same working principle, the joint modules are different in view of mechanical design and have different dimensions and characteristics. Note that torque of the soft rotary actuators is globally proportional to pressure, but also depends on angle.

The R100 has a diameter of D=100 mm and a height of H=80 mm. It has a housing of a cage form, consisting of two cylinders whose relative motion is enabled by using the ultra slim roll bearings. The weight of one chamber is 50 g and the total actuator weight is approximately 500 g, which is a result of the needed mechanical stability. Effective angle working range of the R100 is currently limited to ± 45°, while the maximal torque is 20 Nm developed at the working pressure of 5 bar. The R90-actuator has a diameter of D=90 mm and a height of H=70 mm. This actuator has no housing and its weight is 200 g, while the maximal torque produced by the R90 is 14Nm at a working pressure of 5bar. Angle working range of the R90 is ± 90°. More details on the design of these actuators can be found in [1], [2].

Note that torque of these actuators is characterized by a hysteresis due to viscoelastic properties of the materials used for manufacturing the actuators' chambers.

Two experimental setups representing two application fields of the rotary soft fluidic actuators are considered in this paper: a two-link robot arm and a proof-of-the-concept model of a therapy device for knee rehabilitation.

The robot arm shown in Fig. 1 consists of two R90 modules connected by lightweight links. Each actuator is equipped with an angular encoder, two pressure sensors and two servo valves (GAS-Automation WS 15 G1/8), which are placed at the robot base.

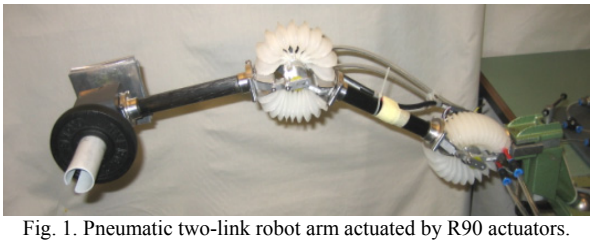

Fig. 1. Pneumatic two-link robot arm actuated by R90 actuators.

A prototype of the device for knee motion therapy is shown in Fig. 2. The device is driven by two R100-actuators connected in parallel aiming to double the actuating torque.

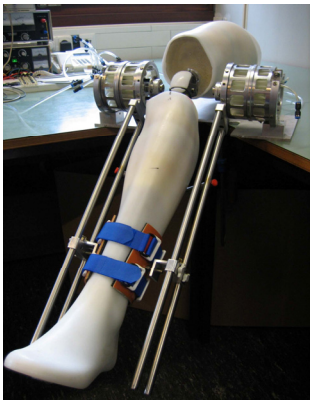

Fig. 2. Prototype of the device for knee motion therapy with R100 soft-actuators.

The set-up is equipped with an angular encoder, two pressure sensors and two servo valves (Festo MPYE-5-1/8LF-010-B).

III. MODELING THE SOFT-ACTUATORS AND VALVES

The physical model of the pneumatic soft-actuators consists of the motion equation of the actuator moving parts, a model of pressure dynamics in the actuator chambers and a valve model. The equation of motion is given as

$$J\ddot{q} = M(p_1, p_2, q) - M_{loss}(\dot{q}, p_1, p_2) - M_{ext} \quad (1)$$

where q is the actuator angle, p_i (i=1,2) are pressures in the chambers, J stands for total moment of inertia with reference to the axis of rotation, M_{loss} represents torque losses, and M_{ext} includes gravitational forces as well as external disturbances. The actuator torque is calculated as a difference of the torques developed by each chamber, i.e. $M = M_1(p_1,q) - M_2(p_2,q)$.

The torque characteristic of the antagonistically coupled elastic chambers is assumed symmetrical with respect to the joint angle and is approximated based on the experimental data, as

$$M_1 = m_1 \cdot q^3 + m_2 \cdot q^2 + (m_3 p_1 + m_4) \cdot q + m_5 p_1 + m_6 \quad (2)$$
$$M_2(p_2, q) = M_1(p_1, -q) \quad \text{for } p_1 = p_2$$

where m_i (i=1..6) are constants. Note that the torque characteristic of these actuators is a nonlinear function of pressure in the actuator chambers, but also of the vane's angular position, while the torque of common single vane fluid motor is proportional to the differential pressure only. Furthermore, this model does not take into account the torque/angle hysteresis. The torque losses M_{loss} are of friction type and are in first approximation measured in the experiments at constant velocities [5].

Besides position dependent torque characteristic, a further specific feature of the REC-actuator is a consequence of its complex volume characteristic, which influence the pressure dynamics in the actuator chambers:

$$\dot{p}_i = \frac{\chi}{V_i}(RT\,\dot{m}_i - p_i \dot{V}_i), \quad i = 1,2 \quad (3)$$

where V_i are the chamber volumes, χ is the polytropic coefficient, R is the universal gas constant, $\dot{m}_i$ are the mass flow rates into or out of the chamber, T is the air temperature. Similar to the torque characteristic (2), the volume characteristic of the REC-actuators is assumed to be symmetrical with respect to the joint angle and is approximated based on the experimental data as:

$$V_1(q, p_1) = v_1(p_1)q^2 + v_2(p_1)q + v_3(p_1) \quad (4)$$
$$V_2(q, p_2) = V_1(-q, p_2)$$

$v_j(p_1)$, j=1,2,3, are polynomials for pressure values with $p_1 \in [1,6]$ bar. Note that the volume characteristic of the actuators is a nonlinear function of the actuator angle and also of the corresponding pressure in the chamber, while for a conventional vane actuator the chamber volume is linearly proportional to the angle only.

The mass flow rate of air through the valve is usually

described by the model of air flow through an orifice.

To provide more exact model of the valves and to take into account the hard nonlinearities as the dead-zones, we use an experimental procedure to obtain the relationship between the air flow, up- and downstream pressures and the input voltage to the valve:

$$\dot{m}_i = f(u_i, p_{iu}, p_{id}) \cdot \quad (5)$$

The experimentally determined characteristic of the Festo servo valve is shown in Fig. 3.

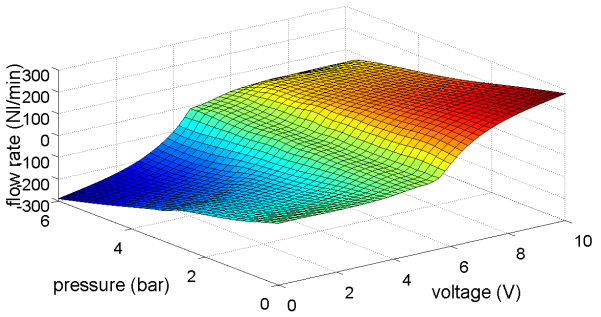

Fig. 3. Experimentally determined flow map for the valve Festo MPYE-5-1/8LF-010-B.

The equations (1-5) build the mathematical model of the considered systems.

IV. PRESSURE CONTROL SUBSYSTEM

To compensate for already mentioned pressure subsystem nonlinearities, as well as to decouple the pressure subsystem from the mechanical subsystem a control law is derived using feedback linearization approach [5]. In the first step the flow rate is chosen as:

$$\dot{m}_{id} = \frac{V_i}{\chi RT}\left(\dot{p}_d + K_p(p_d - p_i) + \chi \frac{dV_i}{dt}\frac{1}{V_i}p_i\right) \quad , \quad i = 1,2 \quad (6)$$

where $\dot{m}_{id}$ as desired flow rate into an actuator chamber and p_d representing the desired pressure in the chamber.

In (6) K_p is the controller parameter of the differential pressure error, which determines pressure controller performance.

The desired flow rate resulting from (6) has to be supplied by the used valves. In this case the flow rate through the used servo valves is directly dependent on the applied control voltage. Thus in the second step, for the determined flow rate the control voltage is obtained by inverting the flow map (5).

To verify the pressure controller performance for both experimental setups, different test settings were applied. First positive and negative step references in the interval of $p_d \in [1,5]$ bar have been applied to the pressure control loop. In a second step the bandwidth is tested, via tracking of a sinusoidal reference pressure. All measurements have been performed at constant chamber volume, achieved through clamping of the moving vane at q=0°. The volume is considered to be constant, because the chambers expand due to their design mainly in median and not in radial direction.

Fig. 4 shows step responses of a R90-actuator with GAS Automation valves, to given desired changes in reference. The step responses are critically damped, with a homogeneous performance in case of positive and negative step references. Over- and undershoot is caused by the GAS

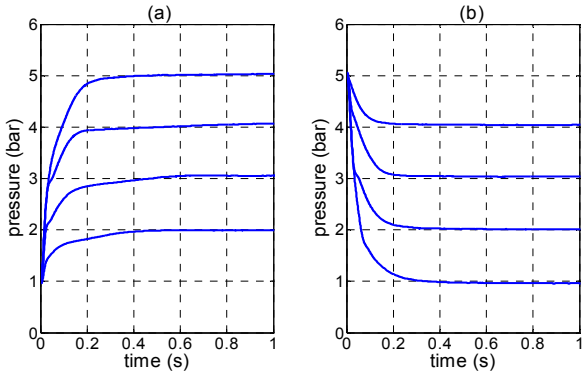

Fig. 4. Closed loop response of R90-actuator with GAS servo valves to (a) positive desired pressures; (b) negative desired pressures.

valves which have no hard closing, when they reach the desired pressure.

Fig. 5 shows performance of pressure control for a R100-actuator with Festo servo valves. Compared to the performance of the R90-actuator setup, the R100 experimental setup shows far better results with a homogeneous performance in all tested cases. Settling times, over- and undershoot as well as steady state errors are smaller. This can be explained through better valve characteristics of used Festo valves, being able to supply a larger flow rate plus the possibility of hard closing.

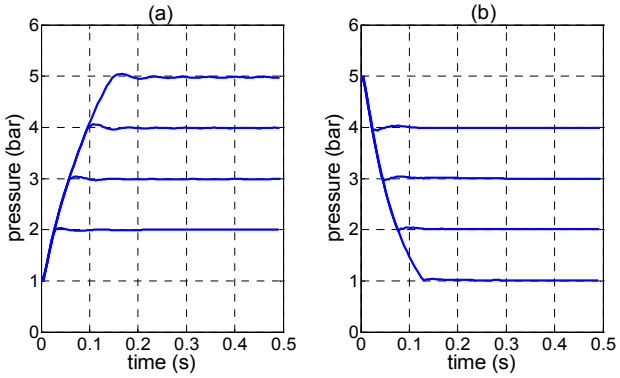

Fig. 5. Closed loop response of R100-actuator with Festo servo valves to (a) positive desired pressures; (b) negative desired pressures.

The behavior of pressure control for variable chamber volumes of the R90 and R100 can be seen in Fig. 6. Table I sums up the specific values of the presented results for the pressure control algorithm (6).

TABLE I
SPECIFIC VALUES OF PRESSURE CONTROL FOR BOTH PRESENTED EXPERIMENTAL SETUPS

setup	t_s (s)	e_{ss} (mbar)	bandwidth (Hz)
R90 & GAS	≤0.37	≤80	3
R100 & Festo	≤0.12	≤20	7

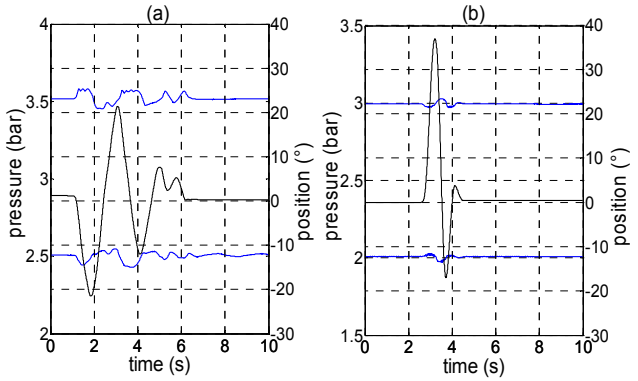

Fig. 6. Performance of pressure control for variable chamber volumes black: actual angular position, blue: pressures of both chambers driving one actuator; (a) R90 with GAS valves; (b) R100 with Festo valves.

V. POSITION CONTROL SUBSYSTEM

Position control of soft-fluidic actuators is due to their nonlinear features a complicated task. Several control schemes provide robust control of nonlinear plants, but require detailed plant model. Controllers presented in this section do not need exact dynamic model of the plant.

A. Sliding Mode Control with Time Delay Estimation (SMCTE)

For position control of the given experimental setups a synthesis of sliding mode control (SMC) and time delay control (TDC) is used. SMC enables control of a nonlinear system in presence of model uncertainties, parameter fluctuations and disturbances [7]. Despite these advantages, SMC needs a detailed nominal model of the plant to be controlled. Time delay estimation based on time delay control achieves estimation of nominal plant dynamics depleting the problem of accurate modeling. The resulting control law is called quasi sliding mode control with time delay estimation (SMCTE), developed in [8].

For the used soft fluidic actuators the control law is chosen as

$$u(t) = u_{eq} + u_{sw} \tag{8}$$

$$= u(t-L) + \hat{b}^{-1}[\ddot{q}_d(t) - \ddot{q}(t-L) + \lambda(\dot{q}_d(t) - \dot{q}(t)) - k\tanh(S/\Phi t]$$

where u_{eq} is the time delay estimation of the equivalent control , u_{sw} is the continuous approximation of switching control, $S(e,t) = \lambda e + \dot{e}$ is the sliding surface, e=q-q_d is the tracking error, the time delay L is chosen to be the sampling time T_s and λ, k, and Φ are the controller parameters. In order to estimate the value of the constant control gain $\hat{b}$, an identification experiment was performed, see also [5].

To avoid chattering of the SMCTE controller, a continuous approximation of the saturation function instead of the sign-function is used. The only measured variable in the control law (8) is the actuator angular position q. The actuator velocity and acceleration are computed using numerical differentiation and low-pass filtering.

Fig. 7 shows responses of the prototype device for knee motion therapy with Festo valves to smooth step-like references. The attached load is L= 3.6kg at a distance of 0.21m to the actuator axis. Desired angular end position is given via a smooth step-like trajectory, providing better controller performance. This is obvious, realizing that the controller uses information about velocity and acceleration of desired position trajectories.

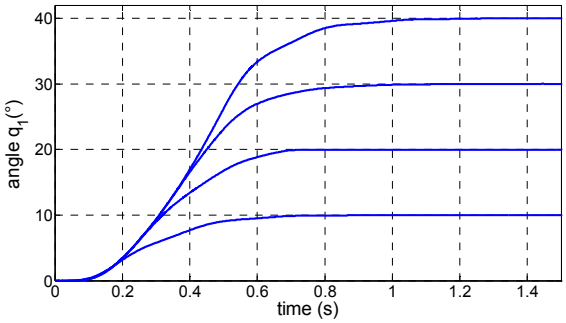

Fig. 7. Position responses of the prototype device for knee motion therapy with SMCTE controller.

In Fig. 7 responses of the soft-actuated prototype device are critically damped for all desired positions $q_d \in [0,40]°$. The settling time t_s is smaller than 0.9s in all cases, while steady state error is smaller than 0.03°. For negative step-like inputs $q_d \in [0,-40]°$ the position controller behaves completely identical regarding settling times and steady state errors.

To test the bandwidth of the SMCTE algorithm in combination with above mentioned experimental setup, a sinusoidal trajectory with the amplitude of 10° at different frequencies $0.2\text{Hz} \le f \le 1.5\text{Hz}$ is prescribed.

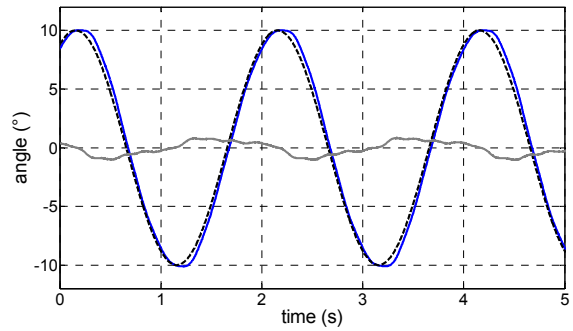

Fig. 8. Trajectory tracking of prototype device for knee motion therapy and SMCTE controller at f=0.5Hz.; desired trajectory (solid line); actual position (dashed line); controller error (grey line).

Fig. 8 exemplary shows controller performance at a frequency of 0.5Hz. It is apparent that the SMCTE algorithm achieves very good trajectory tracking, without remarkable phase shift and a maximum tracking error of 0.8°. A notable breakdown of the closed loop response can be observed for a frequency of f≥1.5Hz. Taking into account, that for knee motion therapy the frequencies about 0.01Hz are usual (for typical velocities from 30° to 200° per minute and maximum motion area 145°), the achieved bandwidth is more than satisfactory.

B. Fuzzy Controller

Fuzzy control has proven to be very successful in the absence of an exact model of the plant. In principal it is possible to create a Fuzzy-Controller solely based on the knowledge of the system's general dynamic behavior. To find satisfying results, however, mostly a process of Trial and Error is needed to "fine-tune" the fuzzy-controller. Unfortunately the before mentioned highly nonlinear characteristics of the REC actuator make it very difficult to judge the systems dynamics making it almost impossible to find suitable results based on this simple approach.

Genetic algorithms (GA) are capable to find optimal solutions for highly complicated optimization problems with a large number of independent variables and are therefore also capable to create or optimize fuzzy controllers. Starting from a randomly generated population of possible solutions for a given problem, genetic algorithms use the mechanisms of evolutionary genetics in order to find optimal results. They apply the "survival of the fittest"-principal in conjunction with a structured but still stochastic data interchange between the single individuals and simulate in that way an evolutionary process. The historical information of this process is continuously evaluated to find new, potentially better solutions for a given optimization problem [10].

For position control of the two-link robot-arm two separate MAMDANI-type fuzzy-PD+I-controllers are used. The controller inputs are position error and velocity, while a separate integral part is added to the controller to eliminate the steady state error. Both inputs and the output are normalized to a range of values of [-1;1] using scaling factors and fuzzificated with seven Gaussian-shaped, evenly spread membership functions.

In order to optimize the fuzzy controllers using genetic algorithms, it is necessary to represent the controller parameters as a series of real numbers. To reduce the number of parameters to be optimized, only the fuzzy rules and the scaling factors (GU_i, GCE_i, GIE_i, GE_i) are optimized via the genetic algorithm – the shape and position of the membership functions as well as the number of fuzzy rules are fixed. It is therefore assumed that all possible combinations of the two controller inputs are needed to control the position of the REC-joints. The creation of the fuzzy rulebase can hence be reduced to the generation of the rules base's conclusions.

As already mentioned, genetic algorithms apply the "survival of the fittest"-principal in order to find optimal solutions. It is therefore necessary to provide a way to judge the performance of every possible solution which is generated by the GA during the optimization process. This is achieved by a closed loop simulation of the current two controllers with a *MATLAB/SimMechanics*-model of the two-link-robot-arm. The overall performance of the current individual is calculated using the following cost function.

$$\text{Performance} = \left(\frac{IAE_{link1} + IAE_{link2}}{2}\right)^{-1} \quad (9)$$

$$\text{with} \quad IAE = \int_{t=0}^{\infty} |q_d(t) - q(t)| dt = \min$$

In (9) q_d is given via a smooth step-like trajectory similar to the SMCTE approach. Fig. 9 exemplary shows the control surface of the optimized controller after 200 generations.

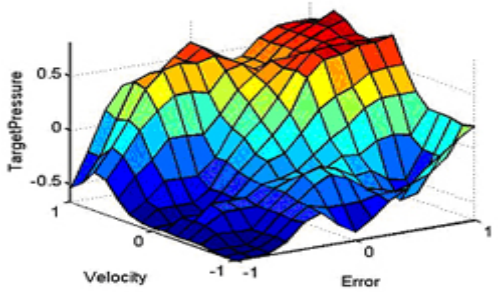

Fig. 9. optimized control surface for the first link's controller

C. Comparison of Experimental Results

In the following experimental results for closed loop position control of a two-link planar robot equipped with R90-actuators are shown. Both presented control algorithms (fuzzy and SMCTE) have been implemented, while a decentralized control scheme is used. Two different series of experiments point out quality of applied control, while the results relate to the robot operating in diagonal plane, with a pitch of 30° with respect to the vertical plane.

Fig. 10 shows the results of the individual joint position control. The attached load is L=0.4kg for all experiments. For the case shown in Fig. 10(a), when both joints are moving upwards, the response of the SMCTE controlled robot is critically damped. For the fuzzy controlled robot there are notable oscillations in transient response, especially at joint 2. For the diagrams in Fig. 10(b), when both joints are moving downwards, similar conclusions for the SMCTE controller can be drawn, while the transient response of the fuzzy controller is oscillating strongly at both joints, resulting in undesirable coupling effects. In spite of these oscillations settling times are identical for both controller types. Note that in case of given positive step-like inputs, steady state errors for the fuzzy controlled actuator are too high with e_{ss}=0.12°. Thus SMCTE provides better steady state behavior and a smoother step response which is quite satisfactory.

Fig. 11 shows the second series of experiments where one of the joints is given a change in reference, while the controller of the second joint should keep the constant position. Movements of single joints result in displacements of the constant kept joints. In case of joint 1 moving up, the SMCTE controller achieves faster disturbance compensation at joint 2 than the fuzzy controller. During movements of joint 2 displacements at joint 1 are compensated almost identically by both controller types.

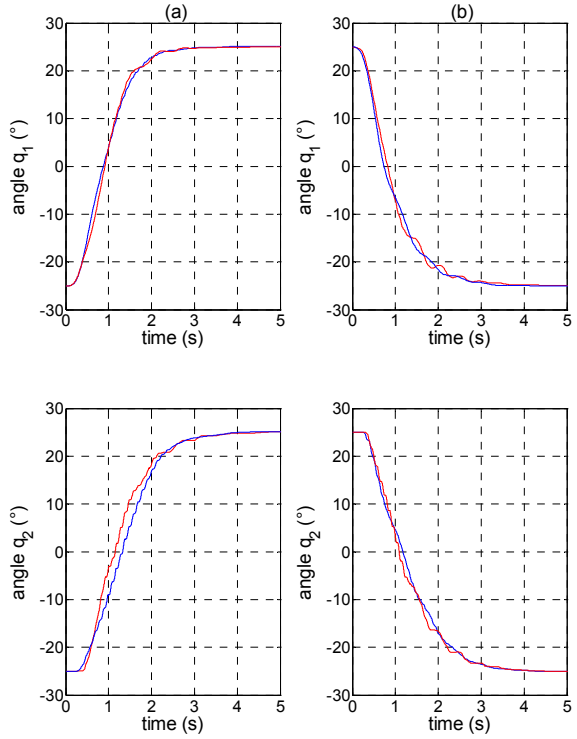

Fig. 10. simultaneous movement of fuzzy (red line) and SMCTE (blue line) controlled two link robot; (a) upwards; (b) downwards.

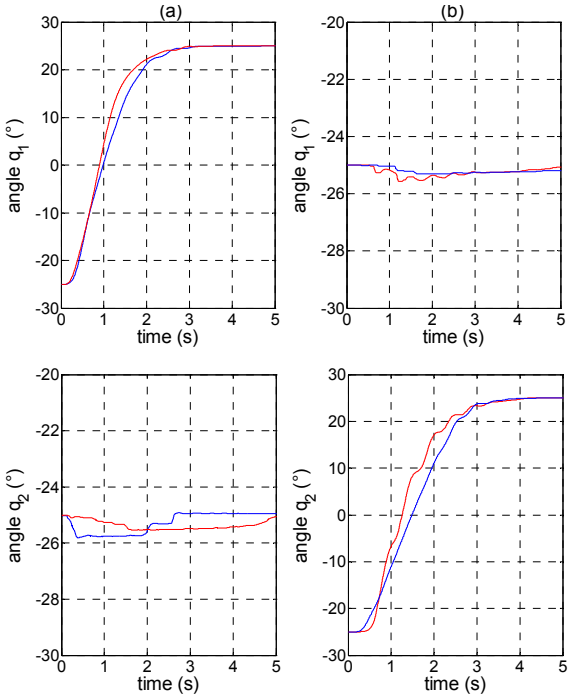

Fig. 11. Experimental position responses for the case when one of the joints is given a change in reference, while the controller of the second one keeps the constant position. (blue line: SMCTE-controller; red line: fuzzy controller); (a) joint 1 moves; (b) joint 2 moves.

VI. CONCLUSION

Exact position control of fluidic soft actuators is due to their nonlinear features a complicated task. Several control schemes provide robust control of nonlinear plants, but require detailed plant model. Controllers investigated in this work do not require exact dynamic model of the mechanical subsystem. Two different position control approaches have been investigated and compared: sliding mode control with time delay estimation as well as a fuzzy control with parameter optimization based on genetic algorithms. Both position controllers have a cascade structure with pressure control in the inner loop. For the pressure control, realized by means of servo valves, the feedback linearization is used.

For individual joint control the satisfactory steady state accuracy smaller than 0.03° within the settling time smaller than 0.9s is achieved using SMCTE algorithm. Also the trajectory tracking performances with maximal tracking error of 0.8° for frequencies about 1Hz are suitable for motion therapy requirements. By decentralized control of the two joint robot arm the SMCTE algorithm shows also better results comparing with the optimized Fuzzy controller. Furthermore, an on-line parameter optimization, as it is often required in robotic applications, is problematically with genetic algorithm due to a long-time optimization process.

ACKNOWLEDGMENT

The of soft robotic joint module R90 was developed and manufactured at the Forschungszentrum Karlsruhe, Institute of Applied Computer Science. The modules of new modification, used in the experimental setup, was made available within the joint research project PortaSoR.

REFERENCES

[1] O. Ivlev, M. Mihajlov, A. Gräser (2006)," Modular multi-sensory fluidic actuator with pleated rotary elastic chambers," *4th IFAC Sym. on Mechatronic Systems*,271-276,Heilderberg, Germany.

[2] A. Kargov, H. Breitwieser, H. Klosek, C.Pylatiuk, S. Schulz,G. Bretthauer (2007),"Design of a modular arm robot system based on flexible fluidic drive elements," *10th Int. Conf. On Rehabilitation Robotics,* 269-73, Noordwijk, NL, June 12-15.

[3] Caldwell, D.; Tsagarakis, N.; Kousidou, S.; Costa, N.; Sarakoglou, Y. "Soft Exoskeletons for Upper and Lower Body Rehabilitation – Design, Control and Testing", International Journal of Humanoids Robotics Vol. 4, No. 3 pp. 549–573, 2007.

[4] T.G.Sugar, et al.," Design and Control of RUPERT: A Device for Robotic Upper Extremity Repetitive Therapy", IEEE Transactions on Neural Systems and Rehabilitation Engineering, vol. 15, no. 3, September 2007,pp. 336-346.

[5] M. Mihajlov, "Modelling and Control Strategies for Inherently Compliant Fluidic Mechatronic Actuators with Rotary Elastic Chambers," Ph.D. thesis, Institute of Automation., Univ. of Bremen., Bremen, Germany, ISBN 978-3-8322-7275-3, 2008.

[6] M.Mihajlov, O. Ivlev, A. Graeser, "Dynamics and Control of a Two-Link Robot Arm with Soft Fluidic Actuators for Assistance and Service Applications,", Robotik 2008, Munich,2008.

[7] J.J Slotine and W . Li, "Applied Nonlinear Control", Englewood Cliffs, NJ: Prentice-Hall, 1991.

[8] Lee HJ, Lee JJ and Kwon DS,"Position control of an SMA actuator using sliding mode control with time delay estimation," *International Journal of Human-Friendly Welfare Robotic Systems*, Vol. 4, No. 2, pp. 51-56, 2003.

[9] J. E. Bobrow and B.W. McDonell, "Modeling, identification, and control of a pneumatically actuated, force controllable robot", *IEEE Trans. Robot. Autom*., vol. 14, no. 5, pp. 732–742, 1998.

[10] D. E. Goldberg,"Genetic Algorithms in Search Optimization and Machine Learning,", Addison-Wesley,1989, ISBN 0201157675